Journal of Applied Polymer Science

Effect of the Molecular Weight between Crosslinks of Thermally Cured Epoxy Resins on the CO_2-Bubble Nucleation in a Batch Physical Foaming Process

Akihiro Ito,[1] Takeshi Semba,[1] Kentaro Taki,[2] Masahiro Ohshima[3]

[1]Department of Organophilic Material Science, Kyoto Municipal Institute of Industrial Technology and Culture, Kyoto 600-8815, Japan
[2]Department of Mechanical Systems Engineering, Yamagata University, Yamagata 992-8510, Japan
[3]Department of Chemical Engineering, Kyoto University, Kyoto 615-8510, Japan
Correspondence to: A. Ito (E-mail: itbba608@kitc.city.kyoto.lg.jp)

ABSTRACT: Epoxy resins (bisphenol A type epoxy resins/2-ethyl-4-methylimidazole) consisting of oligomers with different molecular weights were foamed using a temperature-quench physical foaming method with CO_2. The resulting cell morphologies could be classified into four types: non-foamed structure, cracked structure, star-shaped structure, and sphere-shaped structure. The effects of the gel fraction and molecular weight between crosslinks (M_C) on the cell morphology were investigated for the preparation of microcellular epoxy foams. M_C was calculated by measuring the plateau rubber modulus of the rheological properties and the weight uptake of acetone. By varying the molecular weight of the epoxy oligomers and the cure time, the M_C of the epoxy was controlled to modulate the cell morphology. The experiments elucidated the threshold M_C value that permits CO_2-bubble nucleation: CO_2-bubble nucleation in the epoxy resin could be induced when the distance between the crosslinking points exceeded the critical size of bubble nucleus. Based on this information, the microcellular epoxy foam was prepared by maintaining M_C above 10^4g mol^{-1} and the complex modulus above 6×10^8 Pa. © 2014 Wiley Periodicals, Inc. J. Appl. Polym. Sci. **2014**, *131*, 40407.

KEYWORDS: foams; porous materials; thermosets; crosslinking; swelling

Received 27 August 2013; accepted 9 January 2014
DOI: 10.1002/app.40407

INTRODUCTION

Epoxy resins have many superior properties, such as a high adhesive strength, chemical and heat resistance, high electrical insulation capabilities, high mechanical strength, etc.[1–3] Thus, they have extensive applications, which include coatings, adhesives, composite materials, electrical insulators, and the protection of electrical components from short circuiting due to dust and moisture. Recently, the manufacture of high-end electronic devices has introduced a strong demand for the reduction of dielectric loss on electrical circuit boards. The introduction of air-bubbles into the epoxy-based circuit board is a promising idea to lower the dielectric loss because the dielectric constant of the air is smaller than that of the resin. However, the introduction of these bubbles deteriorates the mechanical properties of the epoxy board. Therefore, micro- or nanocellular foams could be useful in lowering the dielectric property while preserving the mechanical properties of the solid board. The preparation of micro- and nanocellular foams from thermoplastic polymers has been extensively studied.[4–11] Moreover, a reduction in cell size has been verified to improve certain mechanical properties, such as the tensile strength, modulus, strain to failure, impact energy, etc.[12,13] However, few studies have been published on microcellular foams of thermosets, especially epoxy resins. Microcellular epoxy foams can provide high mechanical properties and improve the electrical properties (lower dielectric loss). Epoxy foams have been produced mainly by chemical blowing agents and syntactic foaming, which consists of epoxy resins and porous fillers, such as glass micro balloons.[14–24] The ability of fillers and polymer alloys to improve the flame retardant and mechanical properties has also been tested. The IPN (interpenetration polymer network) of epoxies and polyurethanes,[14] glass fiber- or carbon fiber-reinforced epoxy resins,[15–17] and syntactic foams of epoxy resins[20–22] have also been studied. Simulations of epoxy foams have also reported the heat transfer and heat degradation behaviors of epoxy foams,[23] as well as the compressive strength properties of epoxy foams.[24]

Despite several studies of the applications of epoxy foams, few studies have examined the control of the cell size and foaming mechanism in epoxy resins. Takiguchi et al.[25] investigated the effect of the viscoelastic properties on epoxy foaming. Bisphenol A type epoxy resin was used with 2-ethyl-4-methyl Imidazole as

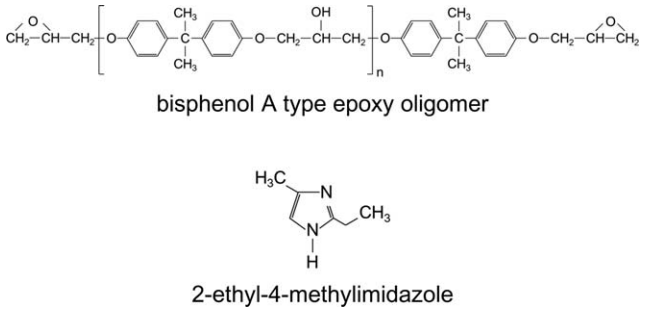

Figure 1. Chemical structure of materials.

the cure agent, and azodicarbonamide (ADCA) was used as a chemical blowing agent to prepare the epoxy foams. Dynamic frequency sweep tests of precured epoxy resins were conducted to determine the critical gelation time. They found that epoxy foams with bimodal cell sizes could be obtained when the epoxy resin was precured before foaming for a time period equivalent to the critical gelation time. Conversely, foams with smaller cell sizes and lower porosities were obtained when the pre-curing time was longer than the critical gelation time. A longer precuring time reduces the size of cells in the foam. A longer curing time maximizes the modulus. However, the epoxy resins that are completely cured cannot be foamed. Determining the optimal curing time is important; it may be a function of the crosslinking structure attributes, such as the gel fraction and molecular weight between crosslinks (M_C). These features are unique properties for thermosetting resins. The relationships between the crosslinking structure and the physical properties are well defined by a number of parameters,[26–31] such as Young's modulus,[28,30] the fracture toughness,[27] the relaxation time,[29] the glass transition temperature (T_g),[29] etc. Increasing the cure time dramatically changes the gel fractions and the crosslinking density of epoxy resins. If cure time is controlled to precisely change crosslinking structures, its effect on the cell morphology can be elucidated through the foam's physical properties.

In this study, we investigated the effects of the viscoelastic properties, gel fraction, and M_C of epoxy resins on the cell morphologies of epoxy resin foams prepared by a batch physical foaming process. Using epoxy oligomers with different molecular weights, epoxy resins with different gel fractions and M_C were prepared by changing the cure time. M_C was calculated from the weight uptakes of acetone and the viscoelastic measurement data. The effect of the complex modulus, gel fraction, and M_C on the cell morphologies was examined.

EXPERIMENTAL

Materials

Three epoxy oligomers (jER828, jER834, and jER1001) with different molecular weights were supplied by Mitsubishi Chemical, Japan. 2-Ethyl-4-methyl imidazole (EMI24 from Mitsubishi Chemical, Japan, melting point = 47–54°C) was used as the curing agent. The chemical structures of the epoxy oligomers and the cure agent are shown in Figure 1. Table I summarizes molecular weights of the epoxy oligomers and average degree of polymerization, which is the number of repeating unit in the chemical structures of the epoxy oligomers. Carbon dioxide (purity = 99.9%, from Kyoto Teisan, Japan) was used as a physical blowing agent. All chemicals were used as received.

Table I. Properties of Three Epoxy Oligomers

	jER828	jER834	jER900
Molecular weight	370 g mol^{-1}	470 g mol^{-1}	900 g mol^{-1}
Average degree of polymerization, n	0.11	0.46	1.97
State of matter (at room temperature)	Liquid	Liquid/solid	Solid

Sample Preparation

The epoxy oligomer and the cure agent were melt-blended by a Planetary Centrifugal Mixer (Series AR-250, Thinky, Japan) at room temperature for jER828 and jER834 and preheated at 130°C for jER1001. The blending conditions for the epoxy oligomer and cure agent are summarized in Table II. The samples prepared from jER828, jER834, and jER1001 are respectively called M370, M470, and M900. The uncured epoxy mixtures were compression-molded by a Hot Press (NF-50, Shinto Metal Industry, Japan) and a silicon rubber-made mold with two disk-shaped cavities that were 25 mm in diameter and 0.5 mm in thickness. The processing temperature was maintained at 70 or 80°C, which was above the melting point of 2-Ethyl-4-methyl imidazole, for 3–120 min. One of two pieces was foamed, and the other sample was used to measure the gel fraction and weight uptake of acetone. Precured epoxy resins with different gel fractions were prepared by changing the compression time (cure time).

CO_2 Dissolution

Two pieces of the samples were placed in an autoclave after measuring the initial weight (W_1). The autoclave was then heated to 35°C. When the temperature reached 35°C, the autoclave was pressurized with CO_2 to 5 MPa. CO_2 was dissolved in the samples by maintaining the pressure and temperature for a given time (24 h for M370 and 60 h for M900). After the given sorption time, the autoclave was depressurized from 5 MPa to the atmospheric pressure within 10 min. The samples were then removed from the autoclave and weighed (W_2). One of the samples was foamed, and the other was used to measure the

Table II. Conditions of Epoxy Oligomer and Cure Agent Blending

Sample name	M370	M470	M900
Epoxy oligmer	jER828	jER834	jER900
Content of 2-ethyl-4-methylimidazole	5 phr	5 phr	5 phr
Preheating temperature	Room temp.	Room temp.	130°C
Mixing time	2 min	2 min	2 min
Degassing time	2 min	2 min	2 min

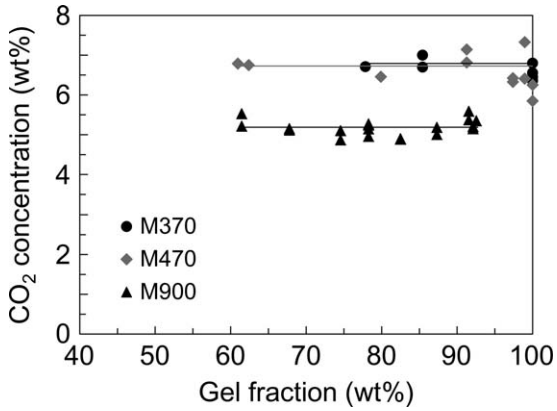

Figure 2. Relationship between the gel fraction and the CO_2 concentration of M370, M470, and M900 (sorption at CO_2 5 MPa and temperature, 35°C).

CO_2 solubility, weight uptake of acetone, and gel fraction. The details of this process are given in the section that describes the characterization of pre-cured epoxy resins.

Physical Foaming

After saturation with CO_2 in the aforementioned sorption process, the pre-cured epoxy resin was heated and foamed by being immersed in oil for 10 s at 90°C. The temperature and the foaming (immersion) time were sensitive to foaming. Lower temperatures and shorter foaming times resulted in insufficient and inhomogeneous foams, i.e. partly foamed and partly non-foamed materials, while higher temperatures and longer foaming times yielded large cells but significantly smaller foam samples. Therefore, the foaming time and temperature were determined by trial and error to generate a well-established and stable cellular structure after removal from the oil bath. To remove the CO_2 from the sample, the foamed sample was maintained at room temperature for 1 day. The sample was then placed in an electronic oven for 4 h at 150°C, which is a standard cure temperature,[32] to complete the curing process. The cell structures of the foamed samples were analyzed by a scanning electron microscopy (SEM5900LV, JEOL, Japan) after sputtering with Au-Pd.

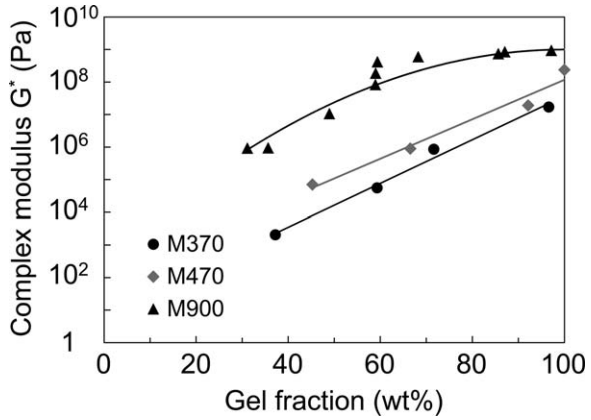

Figure 3. Relationship between the gel fraction and G^* for M370, M470, and M900. (Frequency, 1 Hz; Temperature, 70°C; Geometry, 8 mm ϕ parallel plate).

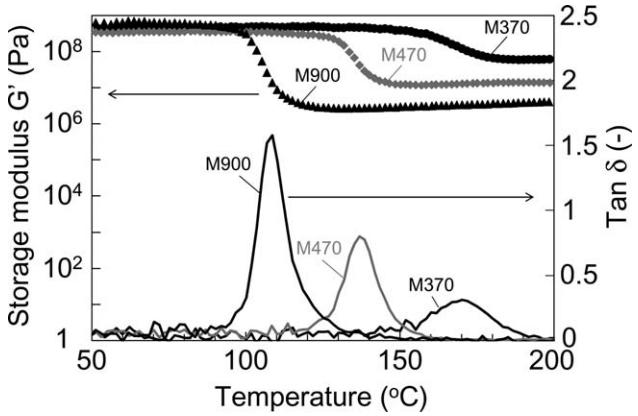

Figure 4. Change in G' and tan δ for a temperature ramp viscoelastic measurement. (Frequency, 1 Hz; heating rate, 10°C min^{-1}; geometry, 8 mm ϕ parallel plate).

Characterization of Precured Epoxy Resins

The amount of CO_2 dissolved in the pre-cured epoxy resin was calculated using eq. (1):

$$(CO_2 \text{ concentration}) = (W_2 - W_1)/W_1 \times 100 \quad (1)$$

The non-foamed sample was soaked in acetone at 23°C for 1 week to measure its gel fraction. The weight of the samples, W_3, was measured after soaking. The sample was dried at 130°C, and the weight of the sample, W_4, was measured after the weight was stabilized. The weight uptake of acetone was calculated using eq. (2)[33]:

$$(\text{Weight uptake of acetone}) = W_3/W_4 \times 100 \quad (2)$$

The gel fraction of the pre-cured epoxy resin was calculated using eq. (3):

$$(\text{Gel fraction}) = W_4/W_1 \times 100 \quad (3)$$

Viscoelastic Measurement

Dynamic time sweep tests were conducted using a rheometer (ARES, Rheometric Scientific, USA) to measure changes in the complex modulus (G^*) during the curing reaction at 70°C and observe the curing behavior of the uncured epoxy mixtures. The measurements were performed using an 8-mm parallel plate geometry and 1 Hz frequency. The auto-strain option was used, and the initial strain of 1% decreased automatically when the torque reached a preset value. The tests were stopped when G^* reached a certain value, following measurements of the sample weight (W_1).

Dynamic temperature ramp tests were also conducted to measure the rubbery plateau modulus of completely cured epoxy resin (G_N^0). G_N^0 was the storage modulus in the plateau region at temperatures above T_g. The temperature was swept from 35 to 200°C using an 8-mm parallel plate geometry at a frequency of 1 Hz and a heating rate of 10°C min^{-1} with a strain of 0.03%.

M_C was calculated from the measured G_N^0 using eq. (4).[34,35]

$$M_C \approx \frac{3\rho RT}{G_N^0} \quad (4)$$

where ρ is the density of epoxy resins, R is the gas constant, and T is the temperature.

Table III. Measured and Calculated Properties of Cured Epoxy Resins

Sample	Molecular weight of epoxy oligomer (g mol^{-1})	G^0_N (Pa) (at 200°C)	M_C (g mol^{-1}) (from G^0_N)	Gel fraction (wt %)	Weight uptake of acetone (wt %)
M370	370	6.2×10^7	229	99.3	102.3
M470	470	1.4×10^7	949	100.0	110.5
M900	900	4.1×10^6	3028	97.1	124.4

In this study, the M_C of completely cured epoxy resin was calculated using eq. (4) with $\rho = 1.17$ g cm^{-3} and $T = 473.1$ K.

RESULTS AND DISCUSSION

The Relationship Between the Gel Fraction and CO_2 Concentration

Figure 2 shows the relationship between the CO_2 concentration and the gel fraction for M370, M470, and M900. The gel fraction correlated positively with the cure time. The solubility of CO_2 was not changed by the gel fraction, but it was changed by the chemical structure. The CO_2 concentrations in M370 and M470 were ~7 wt %, while that in M900 was ~5 wt %. As illustrated in Table I and Figure 1, the degree of polymerization and fraction of hydroxyl groups is higher in M900 than in the other resins. The hydroxyl group is hydrophilic, while CO_2 is a hydrophobic molecule. The CO_2 solubility was decreased when the fraction of hydroxyl groups in the epoxy oligomer was larger. Therefore, the CO_2 solubility was expected to be lower in M900 than in the other resins. The CO_2 concentration was almost independent of the gel fraction because the epoxy group and ether group have a similar hydrophilicity. Therefore, the formation of cross-links negligibly affects the CO_2 solubility.

Characterization of the Gel Fraction and Complex Modulus of Precured Epoxy Resins

Figure 3 shows the complex moduli, G^*, of the pre-cured samples (M370, M470, and M900) as a function of the gel fraction. In general, G^* correlates positively with the gel fraction for all oligomers. Comparing the G^* values of the three different oligomer samples at the same gel fraction indicates that M900 had the largest G^*, followed by M470 and M370. The molecular weight of the oligomer positively correlated with the complex modulus.

Characterization of Crosslinking Molecular Weight of Precured Epoxy Resin

Figure 4 shows the storage modulus, G', and the ratio of the loss modulus to the storage modulus, tan δ, of the completely cured M370, M470, and M900. These materials showed gel fractions of nearly 100%. The apparent glass transition temperature (T_g), at which tan δ is maximized, is clearly observed for each sample. The molecular weight of the epoxy oligomers negatively correlated with T_g and G^0_N. G' decreased from 10^9 Pa to 10^6-10^8 Pa when the temperature was increased above T_g.

The measured G^0_N, M_C, gel fractions, and weight uptakes of acetone are summarized in Table III. The gel fractions of all epoxy resins exceeded 97 wt %, which indicated that the curing reaction was almost completed in all samples. The M_C of the completely cured epoxy resin positively correlated with the molecular weight of the epoxy oligomer.

The effect of the gel fraction on the weight uptakes of acetone is illustrated in Figure 5. The weight uptake of acetone positively correlated with the molecular weight of the epoxy oligomer and negatively correlated with the gel fraction.

M_C could be calculated from the weight uptake of acetone using Flory–Rehner equation[36,37]:

$$M_C \approx \frac{\rho V_0 \left(\nu_2^{\frac{1}{3}} - \frac{\nu_2}{2}\right)}{\nu_2^2 \left(\frac{1}{2} - \chi\right)} \quad (5)$$

$$\nu_2 = \frac{\rho_0}{\rho_0 + \rho\left(\frac{W_3}{W_4} - 1\right)} \quad (6)$$

where ν_2 is volume fraction of the epoxy resins in the swollen samples, ρ is the density of the epoxy resins, V_0 is the molar

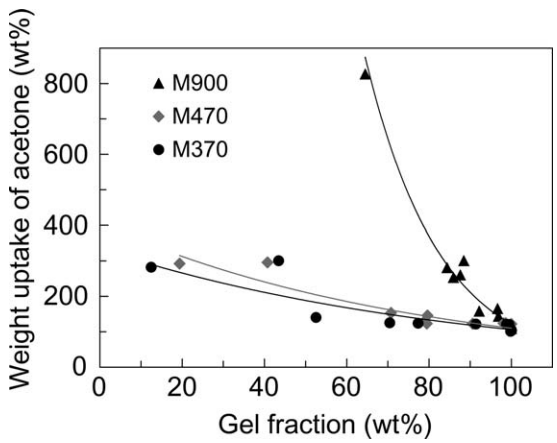

Figure 5. Relationship between the gel fraction and the weight uptake of acetone of M370, M470, and M900.

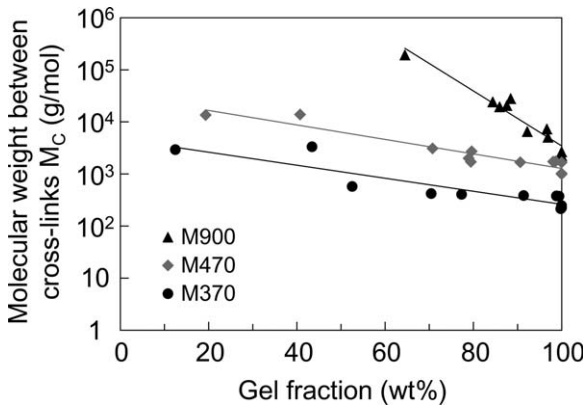

Figure 6. Relationship between the gel fraction and M_C for M370, M470, and M900.

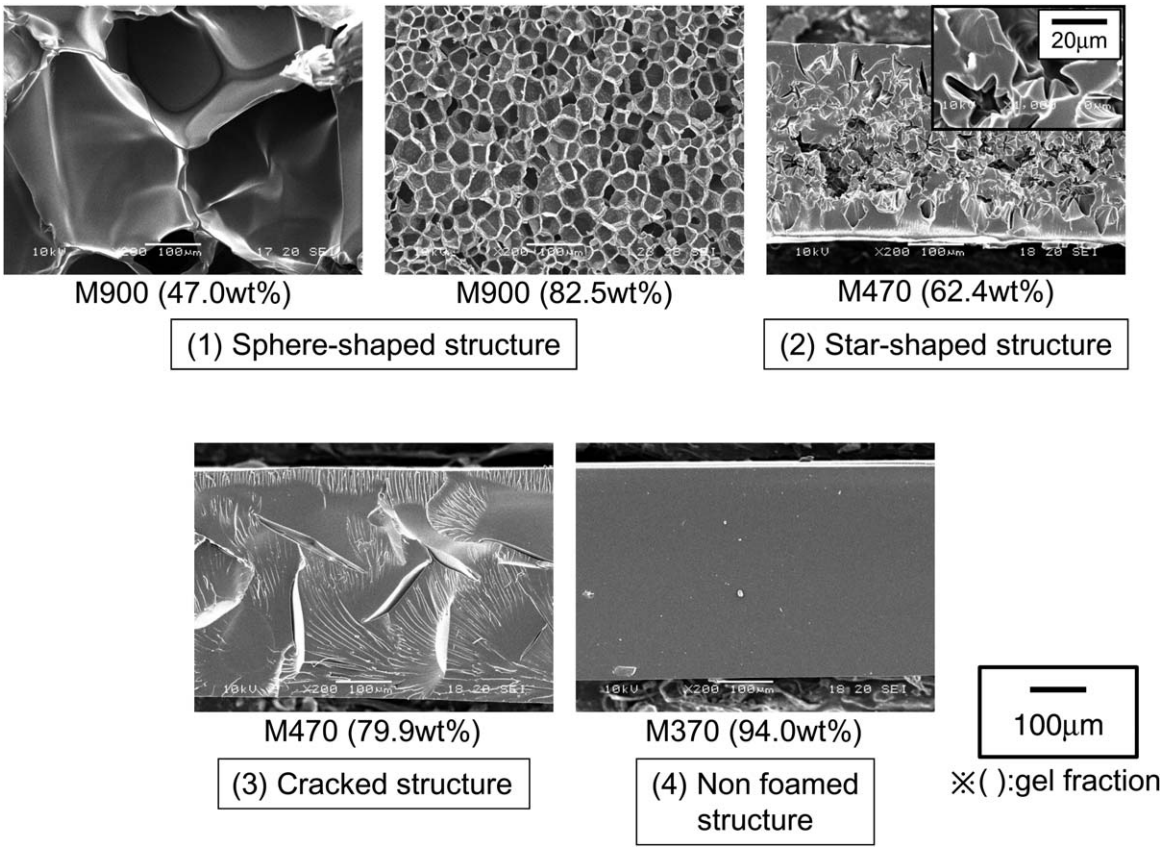

Figure 7. SEM micrographs of cell morphologies of foamed and fully cured epoxy resins.

volume of acetone, χ is the interaction parameter between the epoxy resin and acetone, and ρ_0 is the density of acetone.

χ in eq. (5) is an unknown parameter. Therefore, the M_C and the weight uptake of acetone of the completely cured epoxy resins were used to determine χ. Substituting ρ with 1.17 g cm^{-3}, V_0 with 74.0 cm^3 mol^{-1}, ρ_0 with 0.78 g cm^{-3}, M_C with 229 g mol^{-1}, and the weight uptake of acetone with 102.3% in eqs. (5) and (6) yields a value of 0.29 for χ for M370. Similarly, the χ of M470 was calculated to be 0.43 and that of M900 was calculated to be 0.47. Assuming that χ is independent of the gel fraction, the M_C of the incompletely cured epoxy resin was then calculated using the weight uptake of acetone at each gel fraction and eqs. (5) and (6). The calculated M_C values of M370, M470, and M900 are illustrated in Figure 6 as a function of the gel fraction. M_C positively correlated with the molecular weight of the epoxy oligomer and negatively correlated with the gel fraction.

Effect of Crosslinking Properties on Cell Morphologies

Foaming experiments were conducted for the three epoxy oligomers with different gel fractions. The cell morphologies of the foamed samples are illustrated in Figure 7 and can be classified into the following four types:

1. Sphere-shaped structure: honeycomb-shaped closed cells that are uniformly distributed
2. Star-shaped structure: star-shaped cells connecting the micro bubbles and micro cracks
3. Cracked structure: scattered cracks that are longer than 100 μm
4. Non foamed structure: absence of cells

Table IV shows precuring conditions, gel fractions, foam densities, and cell structures of all the foamed samples. When the cell structure is sphere-shaped structure, cell diameter (equivalent circle diameter) and cell density, which are analyzed from using the SEM micrographs, are also summarized in Table IV. The foam density positively correlated with the gel fraction for M370, M470, and M900 respectively, while the same gel fraction did not lead to the same foam density and cell structure among M370, M470, and M900. The gel fraction negatively correlated with the cell diameter and positively correlated with the cell density for sphere-shaped structures (1).

Figure 8 shows a map of the cell morphology in the G^* and M_C domains (i.e., distance between crosslinking points, which is discussed later). This figure clearly illustrates that the cell morphology depends on M_C. The morphology of structure (4) was non-foamed when M_C was $<10^3$ g mol^{-1}, while structure (3) shows the cracked morphology that resulted when M_C ranged from 10^3 to several times 10^3 g mol^{-1}. A star-shaped structure (2) was obtained when M_C ranged from several 10^3 to 10^4 g mol^{-1}. Sphere-shaped structures (1) were observed when M_C exceeded 10^4 g mol^{-1}. These experimental data indicate that the bubble nucleation mechanism in epoxy resins is determined by M_C.

Table IV. Morphological Characterization of the Foams

Sample	Compression temperature (°C)	Compression time (min)	Gel fraction (wt %)	Foam density (g cm^{-3})	Cell structure	Cell diameter		Cell density
						Average (μm)	SD (μm)	(1/mm^2)
M900	70	15	47.0	0.21	Sphere-shaped	204.3	87.3	19
		20	48.5	0.14	Sphere-shaped	276.4	92.0	11
		25	53.1	0.16	Sphere-shaped	145.7	33.2	42
		30	56.6	0.19	Sphere-shaped	247.5	73.3	13
		50	75.8	0.85	Sphere-shaped	22.8	5.6	1244
		60	74.6	0.33	Sphere-shaped	37.9	12.6	368
		90	82.5	0.36	Sphere-shaped	30.1	9.8	808
	80	3	61.5	0.65	Sphere-shaped	38.8	19.0	370
		30	87.3	0.63	Sphere-shaped	19.3	6.0	1285
		45	91.6	0.79	Sphere-shaped	21.4	5.6	824
		60	92.5	0.82	Star-shaped	-	-	-
		120	100.0	0.91	Cracked	-	-	-
M470	70	40	62.4	0.95	Star-shaped	-	-	-
		50	61.0	0.96	Star-shaped	-	-	-
		60	79.9	1.19	Cracked	-	-	-
		90	91.9	1.18	Non Foamed	-	-	-
M370	70	40	51.9	1.20	Cracked	-	-	-
		50	55.4	1.19	Cracked	-	-	-
		60	77.8	1.21	Non foamed	-	-	-
		90	94.0	1.20	Non foamed	-	-	-
		105	100.0	1.19	Non foamed	-	-	-

When M_C exceeded 10^4 g mol^{-1}, the resultant large G^* value suppressed the bubble growth and reduced the cell size. Therefore, a small cell structure was formed by increasing G* while maintaining M_C larger than 10^4 g mol^{-1}.

The distance between cross-linking points was approximately calculated using M_C and bond lengths to examine the relationship between the size of a cross-linking network and the critical bubble size for nucleation.[38,39] The calculation was conducted as illustrated in Figure 9: the chemical structure of bisphenol A type epoxy resin was assumed to be that given in Figure 1, where the C—C bond length is 1.54 Å, the C—C bond length (benzene ring) is 1.39 Å, and the C—O bond length is 1.43 Å. The length of the repeating unit in a bisphenol A type epoxy resin was then calculated to be 20.22 nm. Because the molecular weight of this repeating unit 284 g mol^{-1}, the distance between the crosslinking points could be calculated by transforming M_C with the length and the molecular weight. The second vertical axis of Figure 8 represents the distances between crosslinking points transformed by M_C. Increasing the distance between

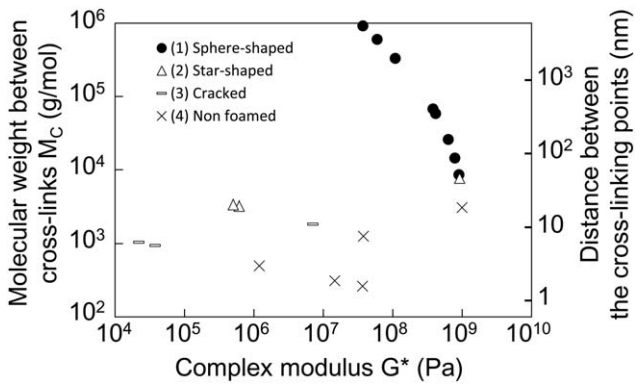

Figure 8. Effect of the gel fraction on the cell diameter and the cell density for the foams with sphere-shaped structure.

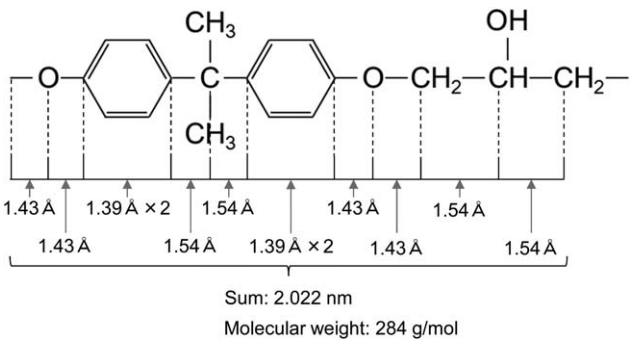

Figure 9. Cell morphologies obtained with different molecular weights of the epoxy oligomer, M_C, and complex modulus.

crosslinking points changed the morphology from a non-foamed structure (4) to a sphere-shaped structure (1). Examining the distance between crosslinking points on the cell morphology map indicates that bubble nucleation could not occur, and nonfoamed cell morphology (4) resulted when the distance was <10 nm. A sphere-shaped structure (1) was formed when the distance between crosslinking points ranged over 50 nm. Following the classical nucleation theory, the critical bubble diameter was calculated as follows[40]:

$$D_C = 2R_C = \frac{4\gamma}{P_D - P_C} \quad (7)$$

where D_C is the critical bubble diameter, R_C is the critical bubble radius, γ is the interfacial tension between a polymer and CO_2, P_D is the pressure in bubbles, and P_C is the atmospheric pressure.

No bubble nucleation were observed in the first stage, which was pressure release using the scanning electron microscopy. The cell nucleation could be observed in the 2nd stage, which was subsequent immersion. Based on the observation of experiments, the critical nucleus size is better to be calculated for the 2nd stage. D_C was calculated to be 31.8 nm by substituting the experimental values P_D =5 MPa and P_C = 0.1 MPa into eq. (7) and using $\gamma = 39$ mN m^{-1} as the reference value of cured bisphenol A type epoxy resins at 60°C.[41] Thus, the range of distances between crosslinking points in which CO_2-bubble nucleation could occur exceeded the values of the critical bubble diameter. The distance between crosslinking points on this map indicated that the bubble nucleation mechanism in epoxy resins requires a distance between crosslinking points that is longer than the critical bubble diameter.

CONCLUSIONS

We investigated the effect of the crosslinking structure on the physical foaming process of epoxy resins. Lower molecular weights of the epoxy oligomer and longer cure times could decrease M_C. The cell morphologies of epoxy foams could be clearly classified into four types: non-foamed structure, cracked structure, star-shaped structure, and sphere-shaped structure. A threshold M_C value was determined for CO_2-bubble nucleation. CO_2-bubble nucleation could be facilitated in epoxy resin when the distance between crosslinking points exceeded the critical size of the bubble nucleus. The complex modulus could control the cell size, even when M_C was sufficiently large to permit bubble nucleation in the epoxy resin. This threshold M_C value for bubble nucleation might be extended to other polymers, where the distance of entanglement points should be larger than the critical bubble nuclei to foam the polymers.

REFERENCES

1. Cassidy, P. E.; Yager, B. J. *J. Macromol. Sci. D* **1971**, *1*, 1.
2. Mostovoy, S.; Ripling, E. J. *J. Appl. Polym. Sci.* **1971**, *15*, 641.
3. Huang, F.; Liu, Y.; Zhang, X.; Wei, G.; Gao, J.; Song, Z.; Zhang, M.; Qiao J. *Macromol. Rapid. Commun.* **2002**, *23*, 786.
4. Colton, J. S.; Suh, N. P. *Polym. Eng. Sci.* **1987**, *27*, 485.
5. Kumar, V.; Suh, N. P. *Polym. Eng. Sci.* **1990**, *30*, 1323.
6. Shimbo, M.; Baldwin, D. F.; Suh, N. P. *Polym. Eng. Sci.* **1995**, *35*, 1387.
7. Arora, K. A.; Lesser, A. J.; McCarthy, T. *J. Macromolecules* **1998**, *31*, 4614.
8. Stafford, C. M.; Russell, T. P.; McCarthy, T. *J. Macromolecules* **1999**, *32*, 7610.
9. Siripurapu, S.; DeSimone, J. M.; Khan, S. A.; Spontak, R. *J. Macromolecules* **2005**, *38*, 2271.
10. Yokoyama, H.; Sugiyama, K. *Macromolecules* **2005**, *38*, 10516.
11. Taki, K.; Waratani, Y.; Ohshima, M. *Macromol. Mater. Eng.* **2008**, *293*, 589.
12. Wei, G.; Jiacheng, G.; Ming, J.; Li, H.; Jie, Y.; Jianhua, Z. *J. Appl. Polym. Sci.* **2012**, *122*, 2907.
13. Miller, D.; Kumar, V. *Polymer* **2011**, *52*, 2910.
14. Zhang, Y.; Hourston, D. J. *J. Appl. Polym. Sci.* **1998**, *69*, 271.
15. Bledzki, A. K.; Kurek, K.; Gassan, J. *J. Mater. Sci.* **1998**, *33*, 3207.
16. Stefani, P. M.; Barchi, A. T.; Sabugal, J.; Vazquez, A. *J. Appl. Polym. Sci.* **2003**, *90*, 2992.
17. Alonso, M. V.; Auad, M. L.; Sorathia, U.; Marcovich, N. E.; Nutt, S. R. *J. Appl. Polym. Sci.* **2006**, *102*, 3266.
18. Alonso, M. V.; Auad, M. L.; Nutt, S. R. *Compos. A* **2006**, *37*, 1952.
19. Auad, M. L.; Zhao, L.; Shen, H.; Nutt, S. R.; Sorathia, U. *J. Appl. Polym. Sci.* **2007**, *104*, 1399.
20. Song, B.; Chen, W.; Yanagita, T.; Frew, D. *J. Compos. Struct.* **2005**, *67*, 279.
21. Gupta, N.; Nagorny, R. *J. Appl. Polym. Sci.* **2006**, *102*, 1254.
22. Devi, K. A.; John, B.; Nair, C. P. R.; Ninan, K. N. *J. Appl. Polym. Sci.* **2007**, *105*, 3715.
23. Hobbs, M. L. *Polym. Degrad. Stab.* **2005**, *89*, 353.
24. Alonso, M. V.; Auad, M. L.; Nutt, S. R. *Compos. Sci. Technol.* **2006**, *66*, 2126.
25. Takiguchi, O.; Ishikawa, D.; Sugimoto, M.; Taniguchi, T.; Koyama, K. *J. Appl. Polym. Sci.* **2008**, *110*, 657.
26. Chang, T. D.; Carr, S. H.; Brittain, J. O. *Polym. Eng. Sci.* **1982**, *22*, 1213.
27. Levita, G.; DePetris, S.; Marchetti, A.; Lazzeri, A. *J. Mater. Sci.* **1991**, *26*, 2348.
28. Urbaczewski-Espuche, E.; Galy, J.; Gerard, J.-F.; Pascault, J.-P.; Sautereau, H. *Polym. Eng. Sci.* **1991**, *31*, 1572.
29. Ogata, M.; Kinjo, N.; Kawata, T. *J. Appl. Polym. Sci.* **1993**, *48*, 583.
30. Urbaczewski-Espuche, E.; Galy, J.; Gerard, J.-F.; Pascault, J.-P.; Sautereau, H. *Macromol. Symp.* **1995**, *93*, 107.
31. Montserrat, S. *Polymer* **1995**, *36*, 435.
32. Perez, R. J. In Epoxy Resin Technology; Bruins, P. F., Ed.; Interscience Publishers: New York, **1968**, 77.

33. Kenyon, A. S.; Nielsen, L. E. *J. Macromol. Sci. Chem.* **1969**, *A3*, 275.

34. Nielsen, L. E.; Onogi, S. Koubunshi no Rikigakuteki Seishitsu (Mechanical Property of Polymer), 1st ed.; Kagaku Doujin Hakkou: Japan, **1965** (in Japanese).

35. Nielsen, L. E. Mechanical Property of Polymer; Reinhold Publishing: New York, **1962**.

36. Shimbo, M. In Epokishi-jushi Handobukku (Epoxy Resin Handbook), 1st ed.; Shimbo, M., Ed.; Nikkan Kogyo Shinbun: Japan, **1987**, 246 (in Japanese).

37. Sperling, L. H. Introduction to Physical Polymer Science, 4th ed.; Wiley: New York, **2006**.

38. Solomon, T. W. G. Organic Chemistry, 6th ed.; Wiley: New York, **1996**.

39. Atkins, P. W. Physical Chemistry, 6th ed.; Oxford University Press: Oxford, **1998**.

40. Gibbs, W. The Scientific Papers of J. Willard Gibbs, Vol. *1*; Dover: New York, **1961**.

41. Abbott, J. R.; Higgins, B. G. *J. Polym. Sci. A Polym. Chem.* **1988**, *26*, 1985.